

The infrared spectroscopy of hydrogen-bonded bridges: 2-pyridone-(water)_n and 2-hydroxypyridine-(water)_n clusters, *n*=1,2

Gina M. Florio, Christopher J. Gruenloh, Robert C. Quimpo, and Timothy S. Zwier^{a)}

Department of Chemistry, Purdue University, West Lafayette, Indiana 47907-1393

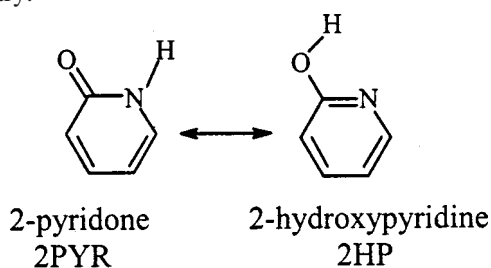
(Received 25 July 2000; accepted 21 September 2000)

The water-containing clusters of the two tautomers 2-hydroxypyridine (2HP) and 2-pyridone (2PYR) are studied in the hydride stretch region of the infrared using the techniques of resonant ion-dip infrared spectroscopy (RIDIRS) and fluorescence-dip infrared spectroscopy (FDIRS). The results on 2PYR-(water)_n build on previous high-resolution ultraviolet spectroscopy [Held and Pratt, *J. Am. Chem. Soc.* **115**, 9708 (1993)] on the *n*=1,2 clusters and the infrared depletion spectra of Matsuda *et al.* [*J. Chem. Phys.* **110**, 8397 (1999)] on the *n*=1 cluster. The 2PYR-W₂ FDIR spectrum reflects the consequences of extending and strengthening the H-bonded bridge between N-H and C=O sites in 2PYR. The spectrum shows evidence of strong coupling along the bridge, both in the form of the hydride stretch normal modes and in the breadth of the observed infrared transitions. RIDIR spectra of the 2HP-W_n clusters are compared with those of 2PYR-W_n in order to assess the spectroscopic consequences of forming the analogous water bridges in the lactim tautomer. Density functional theory calculations are compared with the RIDIR spectra to deduce that the 2HP-W_n clusters are indeed water-containing bridge structures closely analogous to their 2PYR counterparts. The IR spectra of the 2HP-W_n clusters bear a striking resemblance to those of 2PYR-W_n. Potential reasons for the unusual breadth of the bridge XH stretches are discussed.

© 2000 American Institute of Physics. [S0021-9606(00)00347-0]

I. INTRODUCTION

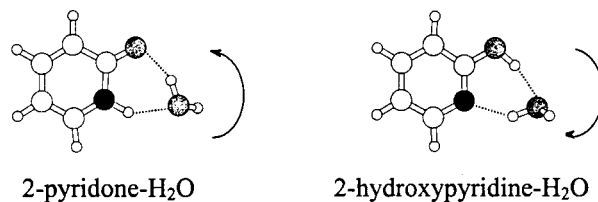
2-pyridone (2PYR) and 2-hydroxypyridine (2HP) are keto-enol tautomers related by transfer of a hydrogen atom between N and O sites in the molecule. As nitrogen heterocycles with the same H-bonding sites as uracil, such tautomerization reactions have potential relevance for proton transport and spontaneous mutagenesis in nucleic acid chemistry.¹⁻⁴



An unusual characteristic of the 2PYR/2HP tautomeric pair is that they are nearly thermoneutral in the gas phase, with 2HP more stable than 2PYR by only 270 cm⁻¹ (0.77 kcal/mol).^{5,6} As a result of this fortunate circumstance, both tautomers are present in significant abundance in gas phase samples (~3:1 in favor of 2HP at 356 K). In solution, their similar stability heightens the importance of solvent effects in controlling the observed equilibrium concentrations of the two tautomers. The less polar 2HP tautomer is favored in nonpolar, aprotic solvents, but 2PYR dominates in polar, protic solvents, including water.³

Not surprisingly, the barrier to tautomerization in the

isolated, gas-phase molecule is substantial, with calculated values of 35–38 kcal/mol.^{7,8} This barrier is reduced to about 13–15 kcal/mol in the presence of a single water molecule bridging the N-H and C=O sites of 2PYR.⁸ As shown below, a bridging water molecule is positioned so that a double H-atom transfer can occur with little heavy atom motion, raising the prospect that tunneling through this smaller barrier could also be significant. Indeed, temperature-jump kinetic studies have provided evidence for a water-mediated proton transfer reaction in solution, though it was unclear from that study whether one or two water molecules were involved in the reaction.⁹ Early calculations employing a small basis set predict a further reduction in the barrier to tautomerization when the bridge is composed of two water molecules rather than one.¹⁰



These attractive features of the 2PYR/2HP tautomers have made them the subject of a number of experimental gas-phase and matrix-isolation studies. A detailed analysis of the infrared spectra of the matrix-isolated tautomers has been carried out by Nowak *et al.*⁶ The microwave spectrum obtained by Hatherley *et al.* determined that 2HP is found exclusively as the *syn* isomer in the gas phase, and determined the relative energies of the 2HP and 2PYR tautomers.⁵ The early resonant ionization and laser-induced fluorescence studies of Tembreull *et al.*¹¹ and Nimlos *et al.*¹² have identi-

^{a)} Author to whom correspondence should be addressed. Electronic mail: zwier@purdue.edu

fied the $S_1 \leftarrow S_0$ electronic origins of the monomers and some of the smaller water clusters. Subsequently, Held *et al.*¹³ carried out an elegant, high-resolution, rotationally-resolved study of the 2PYR-(water)₁, and 2PYR-(water)₂ clusters' $S_1 \leftarrow S_0$ origin transitions. The water molecules in these clusters were shown to form H-bonded bridges between the N-H and C=O groups of 2PYR. In that study, deuterium isotopic substitution was used to determine the positions of the hydrogens in the 2PYR-W₁ bridge.

Recently, Mikami and co-workers¹⁴ have studied the Raman and infrared spectra of 1:1 complexes of 2PYR with a series of solvents, including water. As a part of this study, the IR spectra of partially deuterated 2PYR-water complexes were also recorded in the OH stretch region, establishing the effects of removal of selected OD or ND groups on the infrared spectrum. Finally, Leutwyler and co-workers¹⁵ have recently provided a detailed analysis of the intermolecular transitions present in the vibronic spectra of 2PYR-W_n and 2HP-W_n clusters with $n=1$ and 2.

In this article, we present a study of the ground state infrared spectroscopy of 2PYR-W_n and 2HP-W_n clusters with $n=1$ and 2. The present study builds on previous work in three significant ways. First, the technique of resonant ion-dip infrared spectroscopy (RIDIRS) has been used to record the infrared spectra of the 2HP-W₁ and 2HP-W₂ complexes, which have not been studied previously. These spectra provide evidence that water bridges similar to those present in 2PYR-W_n are also formed in the tautomeric 2HP-W_n clusters. In the case of 2HP, the water molecules bridge between the OH donor and pyridine nitrogen atom acceptor sites. Second, the analogous spectrum of 2PYR-W₂ has also been recorded using fluorescence-dip infrared spectroscopy (FDIRS) to complete the comparison of the water bridges in the two tautomers. Finally, density functional theory calculations of the structures, harmonic vibrational frequencies, and infrared intensities have been carried out on all four clusters to compare with experiment. The vibrational frequency calculations provide insight to the nature, strength, and spectroscopic consequences of the strong coupling present in the H-bonded bridges.

Part of the initial motivation for this study was to search for spectroscopic evidence for water-mediated tautomerization in the hydride stretch infrared spectra of these clusters. Since the hydride stretch normal modes involve motion of the hydrogen atom(s) in the bridge, one might anticipate a close relationship between the in-phase stretching of the bridge XH groups and the water-mediated tautomerization reaction coordinate. The magnitudes of the calculated barriers (~ 4500 cm⁻¹ for 2PYR-W₁)⁸ are similar to the energy provided by excitation of the hydride stretch fundamental. Even below the barrier, the 2PYR-W_n and 2HP-W_n hydride stretch vibrations probe the barrier to tautomerization (i.e., proton transfer) from both "reactant" and "product" sides. Finally, even in the absence of effects due to reaction, the study of the H-bonded bridges formed between the H-bond donor and acceptor sites in 2PYR and 2HP is intriguing in its own right. There is growing evidence that such H-bonded bridges will be both important and pervasive in

solute-(solvent)_n clusters containing multiple, H-bonding sites.¹⁶⁻¹⁸

As we will see, the same sized clusters of 2HP-W_n and 2PYR-W_n have hydride stretch infrared spectra which closely resemble one another. In addition, the hydrogen bonded bridges, particularly in the X-W₂ clusters, produce hydride stretch fundamentals that are several times broader than those of any other X-W₂ clusters studied previously.

II. METHODS

The infrared spectra reported in this work were recorded using the double-resonance schemes of resonant ion-dip infrared spectroscopy (RIDIRS)¹⁹⁻²⁴ and its fluorescence-based analog, fluorescence-dip infrared spectroscopy (FDIRS).^{14,20,25} In both RIDIRS and FDIRS, the population of the cluster of interest is monitored by fixing the ultraviolet laser to a vibronic transition of the cluster, creating a steady-state signal which reflects the ground state population of the cluster of interest. The infrared spectra are recorded by preceding the ultraviolet pulse with an infrared pulse which, when resonant with an infrared transition, removes population from the ground state. The absorption is then detected as a dip in the ion signal or fluorescence generated by the ultraviolet laser pulse that follows.

The data on the 2HP-W_n clusters employed RIDIRS, since its $S_1 \leftarrow S_0$ transition is just over half way to the ionization threshold, and can thus be studied conveniently using one-color resonant two-photon ionization. The molecular beam time-of-flight mass spectrometer employed in these studies has also been described previously. Briefly, the molecular clusters are formed by expansion from a 0.8 mm diameter pulsed valve heated to 100 °C and operating at a backing pressure of 2 bar. The unfocused, doubled output of a Nd:YAG-pumped dye laser (Rhodamine 575 dye) is used as ultraviolet light source. An infrared parametric converter (Laser Vision) pumped by the seeded output of a second Nd:YAG laser (Continuum 7020) is used for the infrared excitation step. It counterpropagates the ultraviolet laser beam, and is focused by a 50 cm focal length lens to the center of the ion source region of the time-of-flight mass spectrometer. Typical infrared powers of about 5 mJ/pulse are used.

The 2PYR-W_n clusters were studied using FDIRS rather than RIDIRS, largely because the $S_1 \leftarrow S_0$ transition of 2PYR is less than half way to the ionization threshold, complicating its study via R2PI. However, the previous characterization of the 2PYR-W_n clusters by high resolution spectroscopy secures the assignment of the ultraviolet transitions to 2PYR-W₁ and 2PYR-W₂, making mass selection unnecessary. The laser-induced fluorescence (LIF) studies are carried out in a second chamber equipped for LIF detection in a supersonic free jet.²⁵ The ultraviolet light is provided by the doubled output of the Nd:YAG-pumped dye laser operating with DCM dye. The same infrared parametric converter is used for the infrared step in FDIRS as in RIDIRS.

Density functional theory (DFT) calculations employing the Becke3LYP functional^{26,27} with a 6-31+G*(d) basis set²⁸ have been carried out to provide a basis of comparison

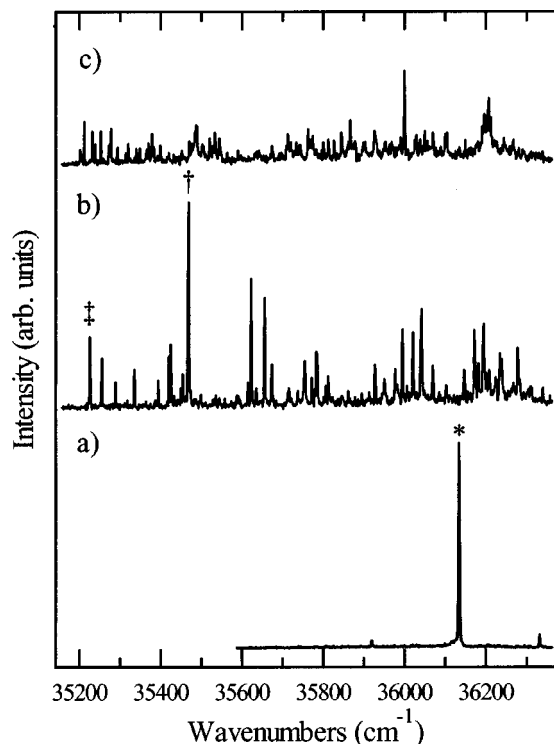


FIG. 1. One-color R2PI scans in the (a) 2HP^+ , (b) 2HP-W_1^+ , and (c) 2HP-W_2^+ mass channels. The * indicates the $S_1 \leftarrow S_0$ origin transition of the 2HP monomer, while † and ‡ label transitions of the 2HP-W_1 and 2HP-W_2 clusters, respectively.

with the experimental results. The fully-optimized structures, binding energies, vibrational frequencies, and IR intensities were computed for various potential structures of 2HP-W_n with $n=1$ and 2. In the case of 2PYR-W_n , only the known,¹³ H-bonded bridge structures were studied. Vibrational frequencies of optimized structures were performed in the harmonic approximation using analytical second derivatives. All calculations were carried out using the GAUSSIAN 98 suite of programs.²⁹

III. RESULTS AND ANALYSIS

A. R2PI of 2HP-W_n

Figures 1(a)–1(c) show one-color R2PI scans near the $S_1 \leftarrow S_0$ origin transition of 2HP while monitoring the 2HP^+ , 2HP-W_1^+ , and 2HP-W_2^+ mass channels, respectively. The monomer mass channel is dominated by the $S_1 \leftarrow S_0$ origin transition of the 2HP monomer, which appears at 36136 cm^{-1} .^{12,15} The largest transition in the 2HP-W_1^+ mass channel at 35468 cm^{-1} (†) has been assigned^{12,15} to the 2HP-W_1 complex. Its large redshift (-668 cm^{-1}) indicates a substantial strengthening of the H-bond between water and 2HP upon electronic excitation of 2HP. Several transitions appear on the low-frequency side of the 2HP-W_1 origin in the 2HP-W_1^+ mass channel. These transitions were also observed by Nimlos *et al.*,¹² but were not assigned. Instead, the transitions that appear in the 2HP-W_2^+ mass channel were assigned to the 2HP-W_2 neutral cluster. In what follows, the 35225 cm^{-1} (‡) transition in the 2HP-W_1^+ mass channel will be reassigned as the 2HP-W_2 $S_1 \leftarrow S_0$ origin transition. The

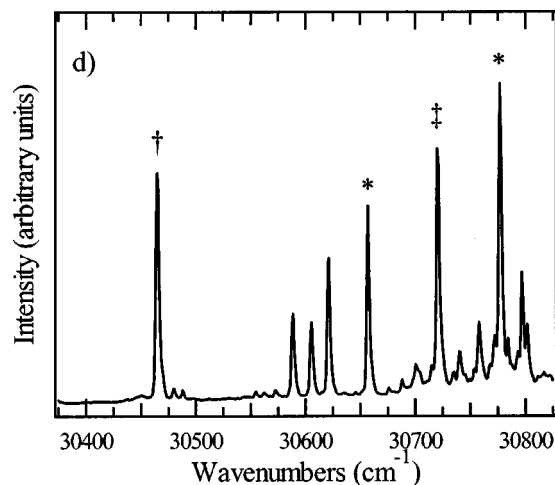


FIG. 2. LIF excitation scan of 2PYR in the region $+500\text{--}900\text{ cm}^{-1}$ from the monomer $S_1 \leftarrow S_0$ origin. The daggers († and ‡) mark the transitions of 2PYR-W_1 and 2PYR-W_2 clusters, respectively. The asterisks (*) designate transitions due to H-bonded dimers of 2PYR.

shift in the 2HP-W_2 origin from the 2HP monomer origin is -905 cm^{-1} , reflecting a 2.60 kcal/mol increase in the total binding energy of the cluster in the S_1 state relative to S_0 . IR–UV hole-burning scans³⁰ (not shown) demonstrate that all the vibronic structure on the low-frequency side of the 2HP-W_1 origin belongs to the 2HP-W_2 cluster. No evidence of these transitions can be found in the 2HP-W_2^+ parent mass channel, indicating that fragmentation by loss of a single water molecule is essentially complete following one-color two-photon ionization at these wavelengths. In contrast, the 2HP-W_1 complex fragments only minimally into the 2HP^+ mass channel. The likely explanation for this change is simply the energetics of the photoionization process, wherein one-color R2PI reaches below the dissociation threshold for $2\text{HP}^+ + \text{W}$ in 2HP-W_1 , but well above the $2\text{HP-W}_1^+ + \text{W}$ threshold in 2HP-W_2 .^{31,32}

B. LIF excitation spectroscopy of 2PYR-W_n

An LIF excitation scan in the region to the blue of the $S_1 \leftarrow S_0$ origin of 2PYR ($30400\text{--}30800\text{ cm}^{-1}$) is shown in Fig. 2. As with 2HP, the previous study of Nimlos *et al.*¹² identified the electronic origins of the 2PYR monomer (29831 and 29930 cm^{-1}) and clusters with one (30465 cm^{-1}) or two (30720 cm^{-1}) water molecules. The latter two transitions are marked with daggers (†, ‡) in the figure. As already mentioned, Held and Pratt¹³ carried out rotationally-resolved LIF studies on these transitions in determining their structures as H-bonded bridges. These transitions serve as the basis for the FDIR spectroscopy reported in Sec. II D.

C. RIDIRS of 2HP monomer and 2HP-W_n clusters and FDIRS of 2PYR-W_n clusters

The RIDIR spectrum of the 2HP monomer (not shown), recorded with the R2PI laser fixed to the $S_1 \leftarrow S_0$ origin at 36130 cm^{-1} [Fig. 1(a)], consists of a sharp OH stretch fundamental at 3598 cm^{-1} and a closely spaced set of aromatic CH stretch transitions in the $3030\text{--}3110\text{ cm}^{-1}$ region. The

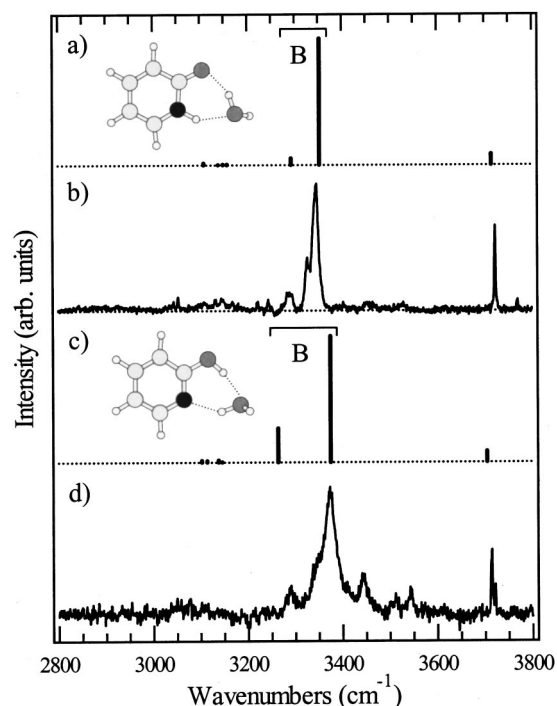


FIG. 3. Experimental (b) FDIR spectrum of 2PYR- W_1 and (d) RIDIR spectrum of 2HP- W_1 compared with the DFT Becke3LYP/6-31+G* calculated harmonic vibrational frequencies (scaled by 0.974) and infrared intensities for (a) 2PYR- W_1 and (c) 2HP- W_1 (A).

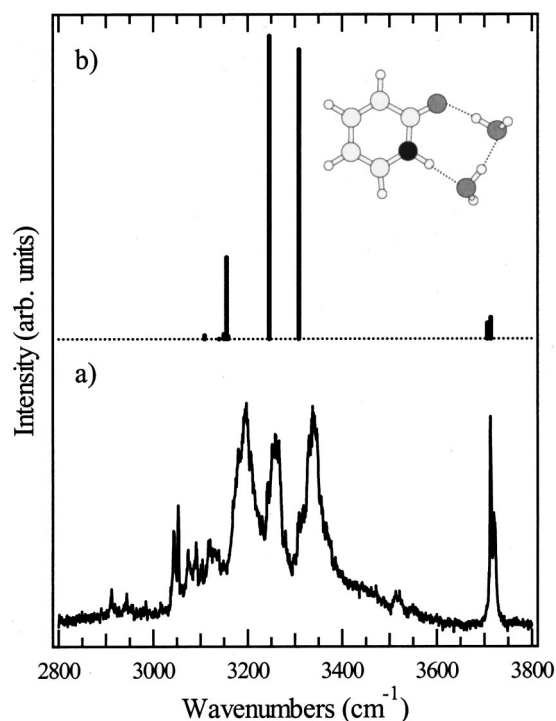


FIG. 4. (a) Experimental FDIR spectrum of 2PYR- W_2 . (b) DFT Becke3LYP/6-31+G*(d) calculated harmonic vibrational frequencies (scaled by 0.974) and infrared intensities 2PYR- W_2 .

frequency of the OH stretch is 59 cm^{-1} lower than that of phenol,²¹ consistent with the assignment of this band to the *syn* isomer, with its weak intramolecular H-bond between the OH and the nitrogen lone pair.^{12,15} The corresponding spectrum of the 2PYR monomer has already been reported in the work of Matsuda *et al.*¹⁴ These authors observe a sharp NH stretch transition for the 2PYR monomer at 3448 cm^{-1} .

RIDIR spectra of 2HP- W_n clusters with $n=1$ and 2 in the OH, NH, and CH stretch region of the IR ($2800\text{--}3800\text{ cm}^{-1}$) are shown in Figs. 3(d) and 5(a), respectively. The corresponding FDIR spectra of 2PYR- W_n are shown in Figs. 3(b) and 4(a). The spectrum of 2PYR- W_1 [Fig. 3(b)] is similar to that already published by Matsuda *et al.*,¹⁴ and is reproduced here primarily for its comparison with 2HP- W_1 . The RIDIR and FDIR scans were recorded by fixing the wavelength of the ultraviolet laser on each of the clusters' origin transitions, marked with daggers in Figs. 1 and 2. The wave number positions and widths (FWHM) of the observed 2PYR- W_n and 2HP- W_n cluster infrared transitions are listed in Tables I and II, respectively.

There are several features of the scans that deserve immediate comment. First, the infrared spectra of 2HP- W_1 and 2HP- W_2 [Figs. 3(d), 5(a)] bear a striking resemblance to their 2PYR counterparts [Figs. 3(b), 4(a)]. This resemblance suggests a similarity in the structures of the clusters, which are known in the case of 2PYR- W_n to be H-bonded bridge structures.¹³ In keeping with this, the sharp transitions due to free NH (3448 cm^{-1} , 2PYR) or free OH (3598 cm^{-1} , 2HP) are absent from the IR spectra, replaced instead by strong, broadened transitions, which appear below 3400 cm^{-1} . This

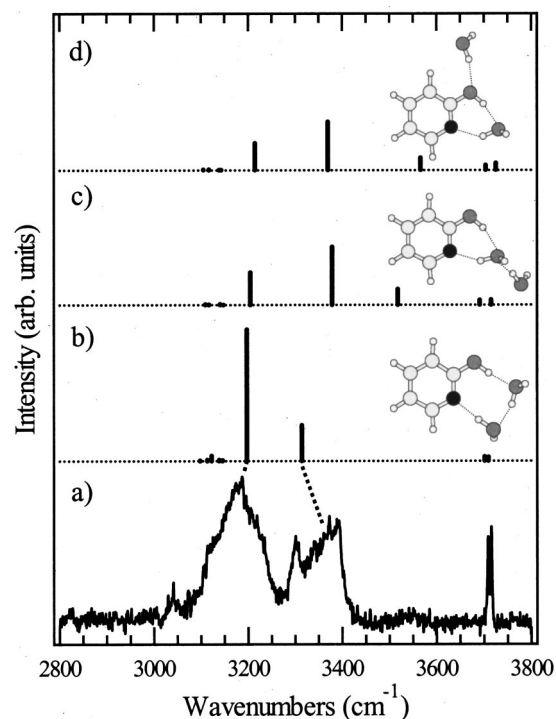


FIG. 5. (a) Experimental RIDIR spectrum of 2HP- W_2 . (b)–(d) Calculated harmonic vibrational frequencies (scaled by 0.974) and infrared intensities for three 2HP- W_2 isomers obtained as minima via DFT Becke3LYP/6-31+G*(d) full geometry optimizations. Structures (B) and (C) are over 5 kcal/mol higher in energy than structure (A). The dotted lines show the assignment of the two H-bonded stretching modes in (b) to the experimental bands in (a).

TABLE I. Experimental vibrational frequencies^a and widths^b for 2PYR- W_n clusters.

2PYR- W_1		2PYR- W_2		Assignment
Freq.	(Width)	Freq.	(Width)	
3770	4			Free OH/Intermolecular bend combination band
3723	4	3721	8 ^c	Free OH
		3713	4	Free OH
3347	15	3337	38	Bridge fundamental
3327	12 ^c			Fermi resonance
3289	16	3258	35	Bridge fundamental
		3195	48	Bridge fundamental
3053	5	3053	4	CH Stretch
3044	4	3043	8	CH Stretch

^aAll frequencies reported in wave numbers (cm^{-1}).

^bThe widths (in cm^{-1}) of the transitions are full widths at half maximum.

^cPartially overlapped band.

is the expected consequence of formation of a water bridge in which the NH (in 2PYR) or OH (in 2HP) groups act as H-bond donors to water. In addition, all four of the water-containing cluster spectra show one or more absorptions in the 3710–3725 cm^{-1} region which can be assigned to free OH groups of the water molecule(s) in the bridge. Second, the relative intensities of the H-bonded bridge fundamentals reflect a degree of coupling between the XH bonds involved in the bridge. For instance, the spectra of 2HP- W_1 and 2PYR- W_1 are dominated by a single H-bonded transition, despite the fact that two H-bonded XH stretches ($\text{OH}\cdots\text{OH}\cdots\text{N}$ or $\text{NH}\cdots\text{OH}\cdots\text{O}=\text{C}$, respectively) make up the single-water bridges in both cases. This point will be taken up further after considering the results of vibrational calculations on the clusters. Third, the H-bonded XH stretch transitions below 3400 cm^{-1} are remarkably broad, especially in the case of the 2PYR- W_2 and 2HP- W_2 clusters

TABLE II. Experimental vibrational frequencies^a and widths^b for 2HP- W_n clusters.

2HP		2HP- W_1		2HP- W_2		Assignment		
Freq.	(Width)	Freq.	(Width)	Freq.	(Width)			
3598	3			3721	2.5	Free OH/tunneling split		
				3714	4	Free OH		
				3716	3	Free OH		
				3708	4	Free OH		
3598	3					OH stretch		
						Bridge fundamentals		
						& intermolecular		
						combination bands		
				3373	34	3372	80 ^c	Bridge fundamental
						3301	27	Fermi resonance
3029	2			3180	120	Bridge fundamental		
				3291	16	Bridge fundamental		
				3041	6	Bridge fundamental		
3045	2.5					CH Stretches		
3054	2.5							
3061	3							
3100	2							
3114	2							

^aAll frequencies reported in wave numbers (cm^{-1}).

^bThe widths (in cm^{-1}) of the transitions are full widths at half maximum.

^cPartially overlapped band.

[Figs. 4(a), 5(a)]. Finally, the signal-to-noise ratio in the FDIR scans [Figs. 3(b), 4(a)] is significantly better than that in the RIDIR scans, due to a greater fluorescence signal in the former case than ion signal in the latter.

D. DFT calculated structures and energies

The low-energy, fully-optimized structures calculated for the 2HP- W_n and 2PYR- W_n clusters with $n=1$ and 2 are shown as insets in Figs. 3–5.³³ The lowest energy structures for all four clusters have been studied in some detail by previous calculations.^{8,10,34,35} The primary motivation for the present calculations is to compute harmonic vibrational frequencies and infrared intensities to compare with the experimental IR spectra. For the 2PYR- W_n clusters, only the known water bridge structures were explored, and the vibrational frequency calculations were used primarily to provide insight to the form of the hydride stretch normal modes and to test the accuracy of the computed vibrational frequencies and infrared intensities against experiment. In 2HP- W_n , where the structures were not known with certainty, several possible H-bonding structures were optimized. Vibrational frequencies and infrared intensities of the minima so-identified then provide a basis for distinguishing the structures observed experimentally.

Table III lists the relative monomer energies and total cluster binding energies, both with and without zero-point energy correction, relative to the 2HP monomer. The labeling scheme used in the table and in Figs. 3–5 reflects the relative binding energies of a given type of cluster with (A) being the calculated global minimum structure followed by (B), etc.

The global minimum structure for 2PYR- W_1 is shown in Fig. 3(a), while that for 2HP- W_1 is shown in Fig. 3(c). Both calculated global minima incorporate water as a bridge between donor and acceptor sites in the two molecules. The H-bonded OH groups are computed to be nearly planar with the ring in both structures, with the free OH of water pointing out-of-plane.

The global minimum structures for 2PYR- W_2 and 2HP- W_2 both consist of distorted water dimers that bridge the H-bonding sites [Figs. 4(b) and 5(b), respectively]. The former structure is essentially that found experimentally from the work of Held and Pratt.¹³ The most remarkable aspect of these structures is the short distance between the two water molecules in the bridge, with oxygen–oxygen separations of only 2.67 Å for 2PYR- W_2 and 2.69 Å for 2HP- W_2 . For comparison, the O–O separation in the water dimer is 2.95 Å³⁶ and in ice I_h is 2.76 Å.³⁷ This short distance reflects the cooperatively strengthened H-bonds in the bridge. In addition, the two H-bonding sites in 2PYR and 2HP appear to be somewhat too closely spaced to accommodate a typical water–water separation, resulting in a “squeezed” dimer. This squeezing is also reflected in changes in the 2HP and 2PYR molecules themselves, most notably in increasing the C–O–H bending angle in 2HP to 114°, nearly 7° larger than its value in the 2HP monomer.

The experimental $S_1 \leftarrow S_0$ origin transition of 2PYR- W_2 is known¹³ to consist of two transitions split by 0.377 cm^{-1} . The rotational constants of these transitions are nearly iden-

TABLE III. DFT Calculated energies for 2-hydroxypyridine and 2-pyridone clusters.^a

Cluster	H-bonded topology	Relative energy ^b		Binding Energy	
		Uncorrected	ZPE corrected ^c	Uncorrected	ZPE corrected
<i>syn</i> -2HP		0.00	0.00		
<i>anti</i> -2HP		5.70	5.44		
<i>syn</i> -2HP-W ₁ (A)	bridge	-11.08	-9.73	11.08	9.73
<i>anti</i> -2HP-W ₁ (B)	chain	-1.74	-1.11	7.44	6.55
<i>anti</i> -2HP-W ₁ (C)	chain	-2.83	-0.21	8.52	5.65
<i>syn</i> -2HP-W ₂ (A)	W ₂ bridge	-23.21	-17.87	23.21	17.87
<i>syn</i> -2HP-W ₂ (B)	W ₁ bridge+ext. W	-17.53	-12.81	17.53	12.81
<i>syn</i> -2HP-W ₂ (C)	W ₁ bridge+ext. W	-16.73	-12.24	16.73	12.24
2PYR		-1.93	-1.74		
2PYR-W ₁ (A)	bridge	-14.21	-11.47	12.28	9.73
2PYR-W ₂ (A)	bridge up/down	-27.83	-22.52	13.62	20.78
2PYR-W ₂ (B)	bridge up/up	-27.11	-21.79	25.18	20.05

^aCalculations performed at the Becke3LYP/6-31+G*(*d*) level of theory. All energies reported in kcal/mol.

^bRelative energy with respect to *syn*-2HP. The absolute uncorrected energy of *syn*-2HP is -202 998.39 kcal/mol.

^cZero-point energy corrections from harmonic frequency calculations at the same level of theory.

tical to one another. Based on the inertial defects of the two transitions, Held and Pratt have suggested that the two structures differ in the nature of the out-of-plane displacements of the hydrogen atoms in the two water molecules.¹³ Based on the calculations, we suggest that the two transitions are tunneling doublets associated with the “up/down” to “down/up” flipping motion,³³ analogous to that found for the free OH groups in the cyclic water clusters.^{38,39} Several less stable local minima have been found for 2HP-W₂, with binding energies at least 5 kcal/mol less than that of 2HP-W₂(A). The structures of two of these clusters (B and C) leave the single water bridge essentially unperturbed, and add the second water to an open lone-pair site on the water or 2HP oxygen, as shown in insets to Figs. 5(c) and 5(d), respectively. An alternative structure, in which the second water accepts a H-bond from the bridging water, has not been investigated because the experimental free OH region [Fig. 5(a)] is inconsistent with an acceptor water molecule (with symmetric and antisymmetric stretches close to that in free water).

E. DFT frequency calculations and the analysis of the infrared spectra

The computed vibrational frequencies and infrared intensities can be used to analyze the experimental infrared spectra in more detail. Throughout this analysis, primary attention will be given to the spectroscopic consequences of bridge formation, highlighting the similarities and differences in the bridges formed in 2PYR and 2HP. The FDIR spectra of 2PYR-W_n clusters with *n*=1 and 2 are compared with the DFT calculated frequencies and infrared intensities in Figs. 3(b)/3(a) and 4(a)/4(b), respectively. The analogous comparisons between the RDIR spectra and theory for 2HP-W_n clusters are shown in Figs. 3(d)/3(c) and 5(a)/5(b). The calculated frequencies and infrared intensities are summarized in Table IV.³³ The harmonic vibrational frequencies were scaled by a factor of 0.974 to correct for anharmonicity.

The scale factor was determined from a best fit of the calculated OH stretch frequencies to the experimental positions for the 2HP-W_n and 2PYR-W_n clusters.

1. The 2PYR-W₁ complex

Since the structure of the 2PYR-W₁ complex is known,¹³ it serves as a good starting point for the analysis. The calculated hydride stretch infrared spectrum of the 2PYR-W₁ complex [Fig. 3(a)] is in quantitative agreement

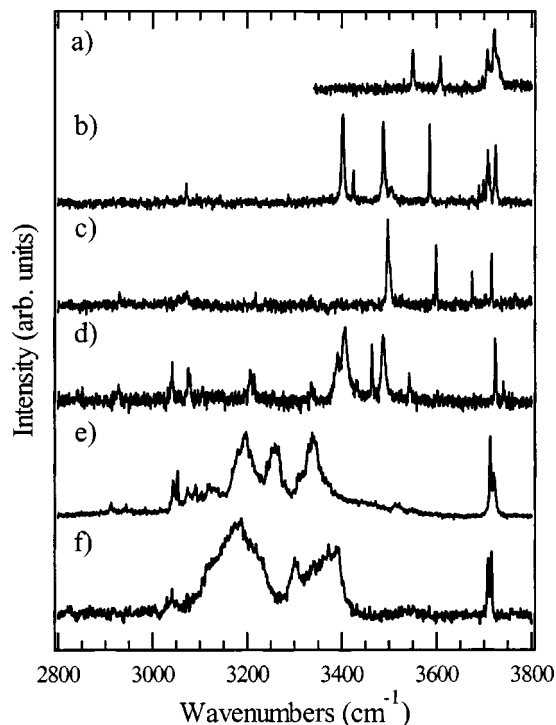


FIG. 6. RIDIR and FDIR spectra of aromatic-W₂ clusters. The aromatic chromophores are (a) benzene, (b) indole, (c) 1-methyl-indole, (d) *trans*-formanilide, (e) 2-pyridone, and (f) 2-hydroxypyridine. Note the increased breadth and large redshift of the H-bonded hydride stretching fundamentals in (e) 2PYR-W₂ and (f) 2HP-W₂.

with experiment [Fig. 3(b)]. Most notably, the DFT Becke3LYP/6-31+G* calculation correctly reproduces the large intensity difference between the two H-bonded bridge fundamentals (labeled with a ‘‘B’’ in the figure) in the 3300 cm^{-1} region. According to the calculation, this intensity asymmetry arises from a strong coupling of the NH and OH motions along the bridge. As Table IV shows, the two vibrations are near-equal mixes of NH and OH oscillation, differing in the phase of oscillation of the bonds. Since the two bonds are nearly antiparallel to one another, the two vibrations lead to constructive (higher frequency) and destructive (lower frequency) interference between the oscillating bond dipoles, thereby collapsing most of the intensity into the higher frequency fundamental. Based on the calculation, the band at 3289 cm^{-1} is tentatively assigned to the weak fundamental. Matsuda *et al.* chose an alternative assignment of the weak fundamental to the shoulder at 3327 cm^{-1} .¹⁴ We prefer an assignment of this shoulder to a Fermi resonance-enhanced combination band involving the carbonyl (1705 cm^{-1}) and C=C (1623 cm^{-1}) stretches, based on the assignment of these fundamentals from the recent FTIR study of matrix-isolated pyridone monomer by Nowak *et al.*⁶

The free OH stretch fundamental at 3723 cm^{-1} is sharp and has an integrated intensity ratio relative to the bridge vibrations that is in excellent agreement with calculation. A weak combination band appears at 3770 cm^{-1} . The narrow width of this band suggests that it is a combination band built off the free OH stretch (F) fundamental (i.e., $F_0^1X_0^1$) involving a 47 cm^{-1} intermolecular vibration X. The frequency of the out-of-plane bend of water (ρ_1) is calculated at 71 cm^{-1} . Since this is the only mode with frequency below 100 cm^{-1} , we tentatively assign the observed combination band as an $F_0^1(\rho_1)_0^1$ combination, despite the rather poor agreement between the calculated and experimental frequencies for the bend.

2. The 2HP- W_1 complex

It was noted earlier that the RIDIR spectrum of 2HP- W_1 bears a distinct resemblance to that of 2PYR- W_1 . This similarity is also reflected in the calculated stick spectra for the two complexes [Figs. 3(c) and 3(a)], which is not surprising in light of the bridge structure taken up by each. In 2HP- W_1 , the two bridge OH stretch fundamentals (B) are somewhat more localized than their 2PYR counterparts, leading to a greater intensity in the lower frequency band. According to the calculation, the intense, higher frequency fundamental is about 70% water OH and 30% 2HP OH, while the lower frequency mode is its complement (Table IV). This greater intensity, however, is not apparent in the experimental spectrum, making an assignment of the lower frequency bridge fundamental to the weak band at 3297 cm^{-1} tentative. One surmises on this basis that the calculations somewhat underestimate the extent of mixing between the bridge OH groups in 2HP- W_1 .

There are several weak bands that appear on the high frequency side of the 3373 cm^{-1} fundamental. These occur at 3444, 3511, and 3544 cm^{-1} , frequencies too high to be ascribed to 2:1 Fermi resonances involving 2HP modes. The latter two bands are 138 and 171 cm^{-1} above the 3373 cm^{-1}

fundamental, respectively. These separations closely match the frequencies of the in-plane bend and stretch of the water molecule against 2HP, assigned recently by Leutwyler and co-workers based on dispersed fluorescence spectra.¹⁵ As a result, we assign the bands at 3511 and 3544 cm^{-1} as $B_0^1IM_0^1$ combination bands involving one quantum of bridge stretch and one of the intermolecular bend or stretch, respectively. The band at 3444 cm^{-1} is most naturally ascribed similarly as a combination band involving a 71 cm^{-1} fundamental. No such vibration was observed by Leutwyler and co-workers,¹⁵ but the calculations identify the out-of-plane rock (ρ_1) at 70 cm^{-1} (68 cm^{-1} scaled), in excellent agreement with experiment. However, such an assignment would cast some doubt on the assignment made in Sec. E 1 of the out-of-plane rock ρ_1 in 2PYR- W_1 to a frequency of 47 cm^{-1} , since the calculations predict a near-identical frequency for this mode in the two complexes.

Finally, the free OH stretch at 3714 cm^{-1} possesses a weak shoulder at 3721 cm^{-1} , split from the free OH stretch fundamental by only 7 cm^{-1} . No intermolecular vibration possesses such a low frequency, nor are there any 2:1 Fermi resonance possibilities in this frequency regime. One possible explanation is to ascribe the 7 cm^{-1} splitting to an H-atom tunneling motion, probably involving the flipping coordinate of the free OH in a double-minimum potential well with minima located above and below the plane of the ring.

3. 2PYR- W_2

The calculated IR spectrum of 2PYR- W_2 [Fig. 4(b)] shows the anticipated effects of lengthening the water bridge by addition of a second water molecule between the N-H and C=O groups of 2PYR. By comparison to 2PYR- W_1 , the addition of a second bridging water molecule contributes a third bridge fundamental below 3400 cm^{-1} and a second free OH stretch around 3700 cm^{-1} . The calculated spectrum of Fig. 4(b) matches the general features of the experimental FDIR scan well [Fig. 4(a)], consistent with the known bridging structure of 2PYR- W_2 .¹³ The scaled frequencies of the transitions are in good quantitative agreement with experiment, but the relative intensities are not, most notably in underestimating the intensity of the lowest-frequency bridge fundamental relative to the others. This lowest-frequency fundamental involves an in-phase oscillation of the three XH groups in the bridge, but is concentrated primarily in the NH oscillator (Table IV). The relative intensities of the three bridge fundamentals are thus a sensitive function of the relative amplitudes of oscillation of the three XH groups in the bridge.

A complex set of bands due to the CH stretches of 2PYR is observed on the low-frequency side of the bridge fundamentals. These bands have gained intensity by mixing with the hydride stretch vibrations. The complexity of the CH stretch region also points to some Fermi resonant mixing of the CH stretches themselves, probably with overtones of the CH and NH bends.

TABLE IV. DFT calculated^a harmonic vibrational frequencies (cm^{-1}),^b infrared intensities (km/mol), and percent character and relative phase (in parentheses) of oscillation of the XH-stretches for 2PYR- W_n and 2HP- W_n clusters.^c

	Freq.	Intensity	2PYR NH	W(1) OH	W(2) OH
2PYR	3595	73			
	3144	3			
	3136	18			
	3114	11			
	3102	13			
2PYR- W_1	3715	79			
	3353	917	37 (-)	63 (+)	
	3293	48	61 (+)	39 (+)	
	3158	5			
	3149	4			
	3139	1			
	3108	13			
2PYR- W_2 (A)	3714	89			
	3707	66			
	3308	1195	0	59 (+)	41 (-)
	3246	1252	23 (-)	31 (+)	46 (+)
	3159	10			
	3155	344	60 (+)	20 (+)	20 (+)
	3150	21			
	3140	0			
	3109	15			
2PYR- W_2 (B)	3718	97			
	3710	64			
	3323	984			
	3261	1373			
	3167	381			
	3157	13			
	3149	8			
	3139	0			
	3108	15			
	Freq.	Intensity	2HP OH	W(1) OH	W(2) OH
<i>syn</i> -2HP	3595	73			
	3144	3			
	3136	18			
	3114	11			
	3102	13			
<i>syn</i> -2HP- W_1 (A)	3705	92			
	3375	1058	32 (-)	68 (+)	
	3264	284	70 (+)	30 (+)	
	3145	3			
	3138	17			
	3114	12			
	3102	14			
2HP- W_2 (A)	3709	74			
	3701	84			
	3314	688	18 (-)	64 (+)	18 (-)
	3198	2526	39 (-)	7 (+)	54 (+)
	3146	16			
	3139	23			
	3122	102	47 (+)	21 (+)	31 (+)
	3113	24			
	3098	13			

^aCalculated at the Becke3LYP/6-31+G*(*d*) level of theory.

^bFrequencies have been scaled by a factor of 0.974.

^cThe reader is referred to EPAPS (Ref. 33) for the infrared frequencies and intensities of higher energy conformers of 2HP and 2HP- W_n .

4. 2HP- W_2

The RIDIR spectrum of 2HP- W_2 [Fig. 5(a)] is compared with the calculated stick spectra for the three potential isomers of 2HP- W_2 in Figs. 5(b)–5(d). A notable difference between the three calculated structures is that isomers B and C possess a weak H-bond due to the “exterior” water molecule, while isomer A does not. These exterior H-bonds produce XH stretch fundamentals above 3500 cm^{-1} , where no such band exists in the experimental spectrum. Instead, the RIDIR spectrum has all its intense transitions below 3400 cm^{-1} . We surmise on this basis that the experimental spectrum must be due to the bridge structure 2HP- W_2 (A), which is the global minimum according to the calculations (Table III).

An assignment of the bands below 3400 cm^{-1} is facilitated by a consideration of the calculated form of the normal modes for the three H-bonded bridge OH fundamentals. As in 2PYR- W_2 , these normal modes involve substantial oscillation of all three OH groups in the bridge. However, the distribution of motion amongst the three OH groups is not equal. As shown in Table IV, the water–water bridge OH [labeled W(1) OH in the table] contributes most to the highest-frequency mode (64%), while the parallel and antiparallel oscillation of the bridge ends dominates the two lower frequency normal modes. In much the same way as in the 2PYR- W_1 and 2HP- W_1 complexes, parallel oscillation of these bridge ends produces an intensity enhancement in the middle-frequency bridge fundamental, while the antiparallel oscillation leads to a suppression of intensity in the lowest frequency mode.

As the dotted lines in Fig. 5 indicate, based on the calculations a tentative assignment of the entire band centered on 3180 cm^{-1} to the enhanced middle-frequency fundamental can be made. The band at 3380 cm^{-1} is then assigned to the water–water bridge OH. No firm assignment of the weak, lowest frequency fundamental is possible, though the weak band at 3040 cm^{-1} is the most likely possibility. If this assignment for the OH stretch fundamentals is correct, it necessitates that the band at 3300 cm^{-1} be assigned either as an XH/intermolecular combination band built off the 3180 cm^{-1} fundamental, or to a band appearing due to Fermi resonance with the bridge OH stretches. In the latter interpretation, the two water OH bend fundamentals, with scaled frequencies of 1640 and 1655 cm^{-1} are likely candidates for the 2:1 Fermi resonance at 3300 cm^{-1} .

IV. DISCUSSION

A. Hydrogen-bonded water bridges

The FDIR spectra of 2PYR- W_n and the RIDIR spectra of 2PYR- W_n clusters with $n = 1$ and 2 provide spectroscopic signatures for hydrogen-bonded water bridges stretched between adjacent donor and acceptor sites in the two tautomers. The similar over-all appearance of the spectra of the bridged tautomers is a result of a clean division of the normal modes into bridge XH stretches and free XH stretches, with the former appearing several hundred wave numbers lower in frequency than the latter.

The differences that do exist in the region of the bridge fundamentals occur because the bridge mode frequencies and relative intensities depend to some degree on the nature of the bridge termination sites and the degree of coupling between the XH groups in the bridge. Given the 150 cm^{-1} frequency difference between the NH stretch of 2PYR monomer (3448 cm^{-1}) and the OH stretch of 2HP monomer (3598 cm^{-1}), it is somewhat surprising that the calculated form of the normal modes in the water-containing bridges are as similar as they are to one another. As is evident from Table IV, the bridge fundamentals are substantially delocalized over the two or three XH groups that make up the bridge. The relative phases and dominant contributors to the modes are calculated to be similar in the two tautomers.

In the W_1 bridges, the two XH oscillators ($\text{NH}\cdots\text{OH}\cdots\text{O}$ in 2PYR- W_1 and $\text{OH}\cdots\text{OH}\cdots\text{N}$ in 2HP- W_1) are strongly coupled to one another, leading to near-equal mixes of the two XH local modes that constructively and destructively interfere with one another as the phase of the two oscillators is changed.

In the W_2 bridges, the coupled motion of the three bridge oscillators is evident in all three normal modes, with the largest contribution to each one retained in the two tautomers. In going from highest to lowest frequency bridge vibration, the phases of the XH oscillators resemble longitudinal phonons containing two, one, and no nodes, respectively (Table IV). This lowest frequency bridge vibration is the one most closely linked with the water-assisted proton transfer reaction coordinate.

The fact that the donor and acceptor H-bonding sites on 2PYR and 2HP are adjacent to one another makes it possible to form water bridges containing only one or two water molecules. However, more generally, there is growing evidence that sites quite remote from one another can be linked by water molecules forming a bridge between them.^{16–18} The spectroscopic signatures of these longer bridges will be intriguing subjects for future study.

B. The unusual breadths of the bridge fundamentals

Perhaps the most striking feature of the IR spectra, particularly of the W_2 bridges, is the unusual breadth of the bridge fundamentals in this small a cluster. To drive this point home, Figs. 6(a)–6(d) present a sampling of infrared spectra of aromatic W_2 clusters studied in our laboratory for comparison with the 2PYR- W_2 and 2HP- W_2 spectra [Figs. 6(e), 6(f)]. The aromatic chromophores are benzene [Fig. 6(a)],^{40–42} indole [Fig. 6(b)],^{30,43} 1-methyl-indole [Fig. 6(c)],³⁰ and *trans*-formanilide [Fig. 6(d)].⁴⁴ In each case the water molecules form a water dimer, attached to the aromatic molecule via the π -cloud (benzene, 1-methylindole), an NH group (indole), and a C=O group (*trans*-formanilide). Note that the latter two groups are the isolated donor and acceptor sites of 2PYR. The assignment of the *trans*-formanilide- W_2 spectrum to an isomer in which the water dimer is attached at the C=O site has been made previously by the groups of Simons^{17,45} and Cable,⁴⁶ and is readily confirmed from an inspection of the RIDIR spectrum, which shows a sharp, unperturbed free NH stretch of *trans*-formanilide at 3465 cm^{-1} .

The unmistakable conclusion of this comparison is that the 2PYR- W_2 and 2HP- W_2 clusters have hydride stretch fundamentals that are qualitatively broader than the others. In 2PYR- W_2 , these widths are about 40 cm^{-1} , while in 2HP- W_2 they approach 100 cm^{-1} or more. That the individual bands are still assignable by comparison with the harmonic frequency calculations indicates that the hydride stretch fundamentals carry the oscillator strength for the entire broadened band. At issue, then, is a plausible explanation for the dramatic increase in breadth observed. Several possible reasons can be postulated.

1. Congestion from more than one species

If the IR spectra were to contain contributions from two or more species, the increased congestion could lead to an apparent increase in the breadths of the bands. Of course, the strength of the double resonance methods employed here is that multiple species can only contribute to the spectrum if they also contribute to the ultraviolet transition used to monitor the ground state population. This is often not an issue, especially in the supersonic expansion. However, it is an established fact that the $S_1 \leftarrow S_0$ origin of 2PYR- W_2 contains two bands,¹³ unresolved at the ultraviolet laser resolution used in recording the FDIR spectrum. The tentative assignment put forward for this doublet is as a tunneling doublet involving the flipping coordinate of the free OH groups that interconverts up/down and down/up minima. If so, the bridge OH stretches should be only slightly affected by the motion, and cannot contribute substantially to the extreme breadths of the observed bands.

2. H-atom transfer

According to the calculations of Field *et al.*,¹⁰ the barrier for concerted H-atom transfer, which converts 2PYR- W_2 into 2HP- W_2 , is on the same order as the infrared photon used to excite the clusters. As Pate and co-workers have shown recently,^{47,48} infrared excitation above the barrier to isomerization produces mixed states encompassing the full vibrational state density at that energy, including levels with different isomeric character. In the present case, then, one wonders whether the mixed states produced by OH stretch excitation might include tautomer levels in which H-atom transfer has occurred. If the coupling to the reaction coordinate were very strong, one could imagine an increase in the breadth due to this coupling.

Two facts argue against this possibility. First, there is little difference in the breadths of the bridge fundamentals, even though only one of the modes should be strongly coupled to the H-atom transfer reaction coordinate. In both the W_1 and W_2 bridges, the lowest-frequency vibration, with its in-phase oscillation of all oscillators, would be anticipated to be the mode most closely associated with the tautomerization reaction coordinate. Of the four bridges studied here, only the 2PYR- W_2 cluster places substantial oscillator strength in this in-phase oscillator. However, its breadth is very similar to that of the other two bridge fundamentals in 2PYR- W_2 .

Second, we have obtained preliminary spectra of oxindole- W_2 , another *cis*-amide like 2PYR, but one which does not have an energetically-accessible second tautomer which can be reached by H-atom transfer.⁴⁹ As we will report elsewhere, the bridge fundamentals in oxindole- W_2 possess a similar breadth to those in 2PYR- W_2 , leading to the conclusion that a mechanism other than H-atom transfer is responsible for the observed broadening.

3. The bridge itself

It seems most likely, then, that the broadening of the bridge fundamentals is inherent to the water bridge itself. Early infrared studies of hydrogen-bonded complexes recognized that the breadth of an XH stretch fundamental is correlated with the strength of the $XH \cdots Y$ H-bond formed.⁵⁰ Thus, the observed breadths in 2PYR- W_2 and 2HP- W_2 are a response of the bridge XH groups to the formation of particularly strong H-bonds associated with the bridge. Formation of a bridge between donor and acceptor sites on the ring has much the same effect as closing a cycle in the pure water clusters.⁵¹ In so doing, the number of strong H-bonds is maximized. At the same time, the completion of the bridge produces a cooperative strengthening of the H-bonds.⁵² That the 2PYR- W_2 and 2HP- W_2 clusters have large binding energies is immediately apparent from the greater frequency shifts of the bridge fundamentals in these clusters [Figs. 6(e), 6(f)] relative to the other cases studied [Figs. 6(a)–6(d)]. The calculations bear this out. The total, zero-point energy corrected binding energies calculated for 2PYR- W_2 and 2HP- W_2 (20.8 and 17.9 kcal/mol, respectively, without correction for basis set superposition error) yield average H-bond energies per H-bond of about 6–7 kcal/mol. By comparison, the total, ZPE-corrected binding energies of benzene- W_2 ,⁴² indole- W_2 ,³⁰ 1-methyl-indole- W_2 ,³⁰ and *trans*-formanilide- W_2 ⁵³ are all calculated to be less than 13 kcal/mol.

The deeper question, though, is why strengthening the H-bonds in the bridge leads to broadening. There are many examples in which strong H-bonds produce XH stretch fundamentals that are spread over several hundred wave numbers, with extensive substructure appearing underneath the overall band profile.⁵⁰ A proper theoretical description of such spectra has occupied the attention of many groups over the past several decades.^{50,54–60} The growing consensus of such studies is that the overall width and substructure is the spectroscopic manifestation of strong anharmonic coupling of the XH stretch to the $XH \cdots Y$ intermolecular stretch, further complicated by Fermi resonant mixing with overtones of the XH bends.⁵⁸ Our spectra show the beginnings of such a breakup of the spectrum, most notably in the 3300 cm^{-1} band in the 2HP- W_2 spectrum. However, at issue here are the widths of the individual XH stretch fundamentals that make up the bridge. These widths are handled by current theories of strong anharmonic coupling only as a generic, medium-induced damping.⁵⁸ In the gas phase, the cluster itself must provide the bath of states responsible for this damping.

According to Fermi's Golden Rule,⁶¹ the observed breadths of the hydride stretch bands must arise from an average coupling matrix element between the hydride stretch

fundamentals and the background states of about 50 cm^{-1} . The density of these bath states are dominated by the intermolecular modes that stretch and bend the H-bonds in the bridge, but whether the full density of states is involved in producing the large breadth is unclear. Given the unusually short water–water separation in these “squeezed” water bridges, one would anticipate unusually strong mechanical coupling across the bridge as the individual XH links in the bridge expand and contract. Furthermore, the background states involved in the broadening could include states in which one of the H-bonds in the bridge is partially or fully broken. Quantitative theoretical modeling of the potential energy surfaces for the intramolecular and intermolecular bridge coordinates is still needed to put such qualitative arguments on firmer footing.

V. CONCLUSIONS

This article has reported the hydride stretch infrared spectral signatures of the H-bonded bridges formed in 2PYR- W_n and 2HP- W_n clusters. The XH stretch region divides cleanly into free OH stretches due to the dangling OH bonds in the water bridge and bridge fundamentals due to the H-bonded XH groups which make up the bridge. The spectra show evidence of the strong H-bonds in the bridge, both in the large frequency shifts of the bridge fundamentals and in the unusual breadths of these fundamentals. Though these breadths may have contributions from the water-mediated tautomerization reaction, it is more likely that the breadths simply reflect the strong coupling of the bridge XH groups with bath states involving the intermolecular modes that stretch and buckle the bridge.

It is likely that such H-bonded water bridges are important in a variety of situations in which partial water solvation of a solute with multiple H-bonding sites occurs.^{16–18,62} Such bridges have been implicated as important factors in stabilizing protein conformations in solution.⁶³ Their study in isolated, gas-phase clusters offers the opportunity to spectroscopically characterize the bridges as a function of the distance, orientation, and nature of the H-bonding sites on the solute and the number of water molecules in the H-bonded bridge.

The 2PYR- W_n clusters have provided an example of the water bridges linking the N–H and C=O sites of a *cis*-amide functionality. In seeking a fuller understanding of the effects that modifying the *cis*-amide group can have on these bridges, we are pursuing several avenues. To better probe the sensitivity of the bridge spectra to subtle changes in the *cis*-amide configuration, a systematic study of other *cis*-amides is currently being pursued in which the N–H and C=O sites are modified from their configuration in 2PYR.⁴⁹ Secondly, it is of interest to form and study longer H-bonded bridges between remote sites on aromatic solutes. Finally, an analysis of the complex, substructured XH stretch spectra that arise in the double bridges formed in the strongly H-bonded dimers of benzoic acid and oxindole is being pursued.

ACKNOWLEDGMENT

The authors gratefully acknowledge the NSF for supporting this research under Grant 9728636-CHE.

- ¹A. R. Katritzky and J. M. Lagowski, *Advances in Heterocyclic Chemistry* (Academic, New York, 1963), Vol. 1, p. 347.
- ²J. S. Kwatkowski, T. J. Zielinski, and R. Rein, *Adv. Quantum Chem.* **18**, 19 (1986).
- ³P. Beak, *Acc. Chem. Res.* **10**, 186 (1977).
- ⁴G. A. Jeffrey and W. Saenger, *Hydrogen Bonding in Biological Structures* (Springer-Verlag, New York, 1991).
- ⁵L. D. Hatherley, R. D. Brown, P. D. Godfrey, A. P. Pierlot, W. Caminati, D. Damiani, S. Melandri, and L. B. Favero, *J. Phys. Chem.* **97**, 46 (1993).
- ⁶M. J. Nowak, L. Lapinski, J. Fulara, A. Les, and L. Adamowicz, *J. Phys. Chem.* **96**, 1562 (1992).
- ⁷M. Moreno and W. H. Miller, *Chem. Phys. Lett.* **171**, 475 (1990).
- ⁸V. Barone and C. Adamo, *J. Phys. Chem.* **99**, 15062 (1995).
- ⁹O. Bensaude, M. Chevrier, and J.-E. Dubois, *J. Am. Chem. Soc.* **101**, 2423 (1979).
- ¹⁰M. J. Field and I. H. Hillier, *J. Chem. Soc., Perkin Trans. 2* **5**, 617 (1987).
- ¹¹R. Trembreull, C. H. Sin, H. M. Pang, and D. M. Lubman, *Anal. Chem.* **57**, 2911 (1985).
- ¹²M. R. Nimlos, D. F. Kelley, and E. R. Bernstein, *J. Phys. Chem.* **93**, 643 (1989).
- ¹³A. Held and D. W. Pratt, *J. Am. Chem. Soc.* **115**, 9708 (1993).
- ¹⁴Y. Matsuda, T. Ebata, and N. Mikami, *J. Chem. Phys.* **110**, 8397 (1999).
- ¹⁵S. Leutwyler (private communication).
- ¹⁶A. Bach and S. Leutwyler, *Chem. Phys. Lett.* **299**, 381 (1999).
- ¹⁷J. A. Dickinson, M. R. Hockridge, E. G. Robertson, and J. P. Simons, *J. Phys. Chem. A* **103**, 6938 (1999).
- ¹⁸S. Mente and M. Maroncelli, *J. Phys. Chem. A* **102**, 3860 (1998).
- ¹⁹R. H. Page, Y. R. Shen, and Y. T. Lee, *J. Chem. Phys.* **88**, 5362 (1988).
- ²⁰T. S. Zwier, *Annu. Rev. Phys. Chem.* **47**, 205 (1996).
- ²¹T. Ebata, A. Fujii, and N. Mikami, *Int. Rev. Phys. Chem.* **17**, 331 (1998).
- ²²P. Imhof, W. Roth, C. Janzen, D. Spangenberg, and K. Kleinermanns, *Chem. Phys.* **242**, 141 (1999).
- ²³P. M. Palmer, Y. Chen, and M. R. Topp, *Chem. Phys. Lett.* **318**, 440 (2000).
- ²⁴K. Buchhold, B. Reimann, S. Djafari, H. D. Barth, B. Brutschy, P. Tarkeshwar, and K. S. Kim, *J. Chem. Phys.* **112**, 1844 (2000).
- ²⁵R. K. Frost, F. C. Hagemeister, C. A. Arrington, and T. S. Zwier, *J. Chem. Phys.* **105**, 2595 (1996).
- ²⁶A. D. Becke, *J. Chem. Phys.* **98**, 5648 (1993).
- ²⁷C. Lee, W. Yang, and R. G. Parr, *Phys. Rev. B* **37**, 785 (1988).
- ²⁸M. J. Frisch, J. A. Pople, and J. S. Binkley, *J. Chem. Phys.* **80**, 3265 (1984).
- ²⁹GAUSSIAN 98, M. J. T. Frisch, G. W. Schlegel, H. B. Scuseria *et al.*, Gaussian, Inc., Pittsburgh, PA, 1998.
- ³⁰J. R. Carney and T. S. Zwier, *J. Phys. Chem. A* **103**, 9943 (1999).
- ³¹H. Ozeki, M. C. R. Cockett, K. Okuyama, M. Takahashi, and K. Kimura, *J. Phys. Chem.* **99**, 8608 (1995).
- ³²G. Reiser, O. Dopfer, R. Lindner, G. Henri, K. Muller-Dethlefs, E. W. Schlag, and S. D. Colson, *Chem. Phys. Lett.* **181**, 1 (1991).
- ³³See EPAPS Document No. E-JCPSA6-113-003047 for a table of the key structural parameters for 2PYR- W_n and 2HP- W_n clusters, and an addition to Table IV that includes the higher-energy 2HP- W_n structures. Additional discussion of the structures, binding energies, and tunneling doublets in 2PYR- W_2 is also included. This document may be retrieved via the EPAPS home page (<http://www.aip.org/pubservs/epaps.html>) or from <ftp.aip.org> in the directory /epaps/. See the EPAPS homepage for more information.
- ³⁴A. Lledos and J. Bertran, *J. Mol. Struct.* **120**, 73 (1985).
- ³⁵J. E. DelBene, *J. Phys. Chem.* **98**, 5902 (1994).
- ³⁶T. R. Dyke and J. S. Muentzer, *J. Chem. Phys.* **60**, 2929 (1974).
- ³⁷F. Franks, in *Water: A Comprehensive Treatise*, edited by F. Franks (Plenum, New York, 1972), Vol. 1, p. 115.
- ³⁸M. R. Viant, J. D. Cruzan, D. D. Lucas, M. G. Brown, K. Liu, and R. J. Saykally, *J. Phys. Chem. A* **101**, 9032 (1997).
- ³⁹M. Schütz, W. Klopper, H. P. Luthi, and S. Leutwyler, *J. Chem. Phys.* **103**, 6114 (1996).
- ⁴⁰R. N. Pribble and T. S. Zwier, *Science* **265**, 75 (1994).
- ⁴¹R. N. Pribble and T. S. Zwier, *Faraday Discuss.* **97**, 229 (1994).
- ⁴²S. Fredericks, K. D. Jordan, and T. S. Zwier, *J. Phys. Chem.* **100**, 7810 (1996).
- ⁴³J. R. Carney, F. C. Hagemeister, and T. S. Zwier, *J. Chem. Phys.* **108**, 3379 (1998).
- ⁴⁴J. R. Carney, T. S. Zwier, A. Fedorov, and J. R. Cable (unpublished results).
- ⁴⁵E. G. Robertson, *Chem. Phys. Lett.* **325**, 299 (2000).
- ⁴⁶A. V. Fedorov and J. R. Cable, *J. Phys. Chem. A* **104**, 4943 (2000).
- ⁴⁷B. H. Pate, *J. Chem. Phys.* **110**, 1990 (1999).
- ⁴⁸D. A. McWhorter, E. Hudspeth, and B. H. Pate, *J. Chem. Phys.* **110**, 2000 (1999).
- ⁴⁹J. R. Carney, T. S. Zwier, A. V. Fedorov, and J. R. Cable (unpublished).
- ⁵⁰G. C. Pimentel and A. L. McClellan, *The Hydrogen Bond* (Freeman, San Francisco, 1960).
- ⁵¹K. Liu, J. D. Cruzan, and R. J. Saykally, *Science* **271**, 929 (1995).
- ⁵²J. K. Gregory and D. C. Clary, *J. Phys. Chem.* **100**, 18014 (1996).
- ⁵³J. A. Dickinson, M. R. Hockridge, E. G. Robertson, and J. P. Simons, *J. Phys. Chem. A* **103**, 6938 (1999).
- ⁵⁴B. Stepanov, *Nature (London)* **157**, 808 (1946).
- ⁵⁵N. Sheppard, in *Hydrogen Bonding*, edited by D. Hadzi (Pergamon, London, 1959), p. 85.
- ⁵⁶A. C. Legon and D. J. Millen, *Chem. Rev.* **86**, 635 (1986).
- ⁵⁷Y. Marechal, *Infrared Spectra of H-bonded Molecules* (Kluwer, Dordrecht, 1991).
- ⁵⁸O. Henri-Rousseau and P. Blaise, *Adv. Chem. Phys.* **103**, 1 (1998).
- ⁵⁹O. Henri-Rousseau and P. Blaise, *Chem. Phys.* **250**, 249 (1999).
- ⁶⁰D. Chamma and O. Henri-Rousseau, *Chem. Phys.* **248**, 91 (1999).
- ⁶¹G. C. Schatz and M. A. Ratner, *Quantum Mechanics in Chemistry* (Prentice-Hall, Englewood Cliffs, NJ, 1993).
- ⁶²A. Bach, S. Coussan, A. Muller, and S. Leutwyler, *J. Chem. Phys.* **112**, 1192 (2000).
- ⁶³M. Petukhov, D. Cregut, C. M. Soares, and L. Serrano, *Protein Sci.* **8**, 1982 (1999).